



Contents lists available at ScienceDirect

Progress in Oceanography

journal homepage: www.elsevier.com/locate/pocean

Thermal indices of upwelling effects on inner-shelf habitats

Fabián J. Tapia^{a,b,*}, Sergio A. Navarrete^a, Manuel Castillo^{a,c}, Bruce A. Menge^d, Juan C. Castilla^a, John Largier^e, Evie A. Wieters^a, Bernardo L. Broitman^{f,a}, John A. Barth^g

^a Estación Costera de Investigaciones Marinas and Center for Advanced Studies in Ecology and Biodiversity, Pontificia Universidad Católica de Chile, Casilla 114-D, Santiago, Chile

^b Center for Oceanographic Research in the Eastern South Pacific (FONDAP-COPAS), Universidad de Concepción, Casilla 160-C, Concepción, Chile

^c Programa de Doctorado en Oceanografía, Departamento de Oceanografía, Universidad de Concepción, Casilla 160-C, Concepción, Chile

^d Department of Zoology, Oregon State University, Corvallis, OR 97331, USA

^e Bodega Marine Laboratory and Department of Environmental Science and Policy, University of California, Davis, P.O. Box 247, Bodega Bay, CA 94923, USA

^f Centro de Estudios Avanzados en Zonas Áridas, Facultad de Ciencias del Mar, Universidad Católica del Norte, Larrondo 1281, Coquimbo, Chile

^g College of Oceanic and Atmospheric Sciences, Oregon State University, Corvallis, OR 97331, USA

ARTICLE INFO

Article history:

Received 21 July 2008

Received in revised form 16 April 2009

Accepted 16 July 2009

Available online xxx

ABSTRACT

Spatial and temporal variability in regimes of coastal upwelling may have profound effects on the distribution and local dynamics of coastal marine populations and entire communities. Currently available mesoscale indices for upwelling intensity lack the resolution needed to characterize and compare inner-shelf upwelling regimes at small spatial scales (1–10's km), which is often required to test relevant hypotheses in ecology, conservation, and management. We present local, quantitative indices of thermal variability, whose pattern across sites is largely driven by variation in coastal upwelling intensity at scales of few kilometers. Index calculations were based on daily records of *in situ* Sea Surface Temperature [SST], gathered at 30 sites along the Oregon–California coast, and at 25 sites along the coast of northern and central Chile. Several univariate metrics were calculated using daily series of temperature anomalies, and combined to produce a multivariate ordination of sites (Multivariate Upwelling Zone Index of Cooling, MUZIC) that allowed us to compare sites across regions. Multivariate indices calculated for 13 central Chile sites explained 52% and 50% of the among-site variance in corticated algal biomass and growth rate, respectively. Upwelling-induced variability at the scales documented here can have significant consequences on the ecology of coastal ecosystems. The basic data requirements (i.e. SST time series) and the simplicity of calculation make these indices a useful tool to apply at a large number of sites around the world, and to examine the generality of community- and population-level responses to physical forcing.

© 2009 Elsevier Ltd. All rights reserved.

1. Introduction

The coastal ocean plays a key role in ocean productivity and the coupling of marine and terrestrial ecosystems (Mann and Lazier, 1996). Interactions between physical and biological processes in this environment have far-reaching consequences for marine food webs, biogeochemical cycling, and many human activities. Critical stages in the life cycle of many species are completed in coastal habitats, where their survival, dispersal and delivery to appropriate habitats are strongly influenced by transport variability (Pineda, 2000; Pineda et al., 2007).

In eastern boundary current regions, wind-driven upwelling is the predominant transport process influencing spatio-temporal variability in nearshore water properties. This has been described for

the Humboldt, California, Canary, and Benguela current systems (Andrews and Hutchings, 1980; Bernal et al., 1982; Bakun and Nelson, 1991; Strub et al., 1998; Mendelssohn and Schwing, 2002). Alongshore winds drive offshore surface Ekman transport, resulting in an onshore and upward movement of sub-surface, cold, nutrient-rich water near the coast (Lentz, 1992; Longhurst, 1998). This local process is influenced by other larger-scale transport phenomena, including coastally trapped waves (Shaffer et al., 1997, 1999; Hormazábal et al., 2001), inter-annual variability in coastal temperature and stratification (Montecinos and Pizarro, 2005; Ramos et al., 2006), offshore eddies and meanders (Washburn et al., 1993; Hormazábal et al., 2004; Chaigneau et al., in press), and flow-topography interactions (Kirincich et al., 2005; Aiken et al., 2007, 2008).

Bakun (1973) proposed a measure of wind forcing derived from large-scale atmospheric pressure fields in order to index the strength of Offshore Ekman Transport at scales of hundreds of kilometers. This Bakun Index captures the temporal dynamics of upwelling (Pérez-Brunius et al., 2007) and provides a quantitative measure of regional-scale patterns that has proven useful in showing strong links between inter-annual variability in upwelling

* Corresponding author. Address: Estación Costera de Investigaciones Marinas and Center for Advanced Studies in Ecology and Biodiversity, Pontificia Universidad Católica de Chile, Casilla 114-D, Santiago, Chile. Tel.: +56 41 2207284; fax: +56 41 2207254.

E-mail address: ftapiaj@udec.cl (F.J. Tapia).

winds and inter-annual changes in phytoplankton biomass and the recruitment of invertebrates and fish (Cury and Roy, 1989; Botsford et al., 1994; Moreno et al., 1998; Ulloa et al., 2001; Navarrete et al., 2002; Scheuerell and Williams, 2005; Shanks and Roegner, 2007). It has also been useful in showing links between upwelling and ecological pattern at spatial scales significantly greater than 100 km (e.g. Connolly et al., 2001; Navarrete et al., 2002, 2005; Scheuerell and Williams, 2005). However, the Bakun index does not resolve spatial pattern in upwelling at scales smaller than ~100 km and, further, it does not necessarily index water properties, which are modified locally by a number of smaller-scale factors (e.g. bathymetry) and inner-shelf hydrodynamics (e.g. Kirincich et al., 2005; McPhee-Shaw et al., 2007).

Small-scale oceanographic structure is well recognized (Graham and Largier, 1997; Pickett and Paduan, 2003; Narváez et al., 2004; Woodson et al., 2007), and is known to bear a strong relationship with the structure and/or dynamics of coastal benthic populations and communities (e.g. Ebert and Russell, 1988; Menge et al., 1997; Connolly et al., 2001; Wieters et al., 2003; Navarrete et al., 2005, 2008; Broitman and Kinlan, 2006; Diehl et al., 2007). However, such relationship has not been quantitatively established partly because there is a lack of indices to characterize inner-shelf sites based on local regimes of environmental variability induced by coastal upwelling, and by its interaction with smaller-scale processes.

In upwelling systems, temperature is a useful measure of how long a water parcel has been near the surface, and thus it reflects an integration of transport processes that affect nearshore communities. Further, it is known that nutrient concentrations are correlated with temperatures in upwelling regions (e.g. Nielsen and Navarrete, 2004; Wieters, 2005; McPhee-Shaw et al., 2007), and it can be expected that other ecological factors such as phytoplankton abundance (e.g. Marín et al., 2003; Venegas et al., 2008), the spatial distribution of meroplankton (e.g. Poulin et al., 2002; Shanks and Brink, 2005), and growth rates of benthic invertebrates (e.g. Phillips, 2005; Blanchette et al., 2006; Menge et al., 2008) may also correlate with coastal temperature variability. The recent availability of nearshore time-series data on water temperature at many sites (e.g. Helmuth et al., 2006) provides the opportunity to develop a thermal upwelling index that represents the effects of upwelling (and related transport processes) at smaller scales. Thus, it is possible to quantitatively classify sites according to their local regimes of variability in temperature and related physical-chemical properties (e.g. nutrient concentration) that are perceived by coastal communities.

Here we develop indices that resolve small-scale patterns in thermal regimes that are ultimately related to the local modulation of coastal upwelling dynamics. These indices are calculated from time series of *in situ* temperatures measured in shallow nearshore waters. Other work has addressed spatial patterns using satellite data (Santos et al., 2001; Navarrete et al., 2005; Broitman and Kinlan, 2006; Lagos et al., 2007; Venegas et al., 2008), but these analyses are limited by temporal gaps in the data series due to cloud cover and the lack of reliable data in the nearshore. Thermal upwelling indices developed in this paper exhibit strong and coherent spatial structure in nearshore environments, which is expected to show significant skill in explaining spatial patterns in the structure and dynamics of nearshore communities.

2. Materials and methods

2.1. Study sites and datasets

Time series of subtidal temperatures that range from 2 to 10 years in length, and gathered from 1997 to 2008, were analyzed for 25 sites over 8° latitude along the coast of Chile and for 30 sites

over 13° along the west coast of the United States (see Fig. 1 and supplementary information Tables A1, A2). Temperatures were recorded using Stowaway TidBit loggers (Onset Computer Corp., USA), deployed approximately 1 m below Mean Lower Low Water (MLLW) in the shallow subtidal for Chile (Fig. 1d and e), at about MLLW for Oregon and northern California intertidal sites (Fig. 1a and b), and between 3 and 4 m below the surface for inner-shelf moorings off central and southern California (Fig. 1b and c). Sampling intervals ranged between 5 and 30 min. Moorings were deployed within 1 km of shore, at bottom depths of 15–20 m (see <http://www.piscoweb.org/data>).

Temperature data from intertidal Oregon and northern California sites were matched up with tidal water level data, allowing identification and removal of data collected while exposed to air. In addition, to remove data where wave action exposed thermistors to air, differences between adjacent data points were calculated and data were deleted for times characterized by jumps in temperature. Series of quality-controlled data from all sites were low-pass filtered and used to produce time series of daily mean temperature $T(t)$. In this way, temperature fluctuations with tidal and higher frequencies were removed from the data prior to computing daily averages, and without aliasing this high-frequency variability.

Since upwelling is strongly seasonal along the coasts of Oregon–California and Chile (Strub et al., 1998; Venegas et al., 2008), we only used data from the spring–summer upwelling season. The austral upwelling season is defined here as the months of October–March, whereas the boreal upwelling season is defined as the months of April–September. Prior to calculating indices of variability, the mean upwelling-season temperature was calculated for each site. A spatial anomaly (T_r) was calculated for each site as the difference between mean temperature for that site and the mean temperature expected from a linear regression between site-specific mean T and latitude (Tables A1, and A2). This was done to remove latitudinal thermal effects and focus on more regional/local patterns in upwelling strength.

Given that upwelling is dominated by synoptic variability, and that the resultant upwelling-relaxation variability is important for nearshore ecological processes, we developed a synoptic-frequency residual record of upwelling for each site by subtracting a 30-day running mean from the daily time series of $T(t)$. This daily temperature anomaly $T'(t)$ thus removed the longer time scales of variability, and highlighted deviations from mean SSTs without the confounding influence of between-site differences in mean temperature.

2.2. Index calculation

While time-series plots of temperature and temperature anomalies reflect the full detail of variability at a given site, we focused on events with negative anomalies that occurred during periods of upwelling-favorable winds. By formulating metrics of these events, we sought to find a parameter or set of parameters that successfully index sites according to the thermal manifestation of coastal upwelling at local scales. We calculated statistics for event duration and intensity for each site, as illustrated in Fig. 2:

1. *Event duration* D_e . The duration of each cooling event was calculated as the number of days elapsed between the onset of a temperature drop and the subsequent zero-crossing as temperature anomalies returned to positive values.
2. *Cooling rate* CR . The intensity of each cooling event as reflected in the cooling rate, i.e., the slope with which the temperature anomaly drops from a local maximum to a local minimum $\Delta T/d$ where d is the number of days elapsed.

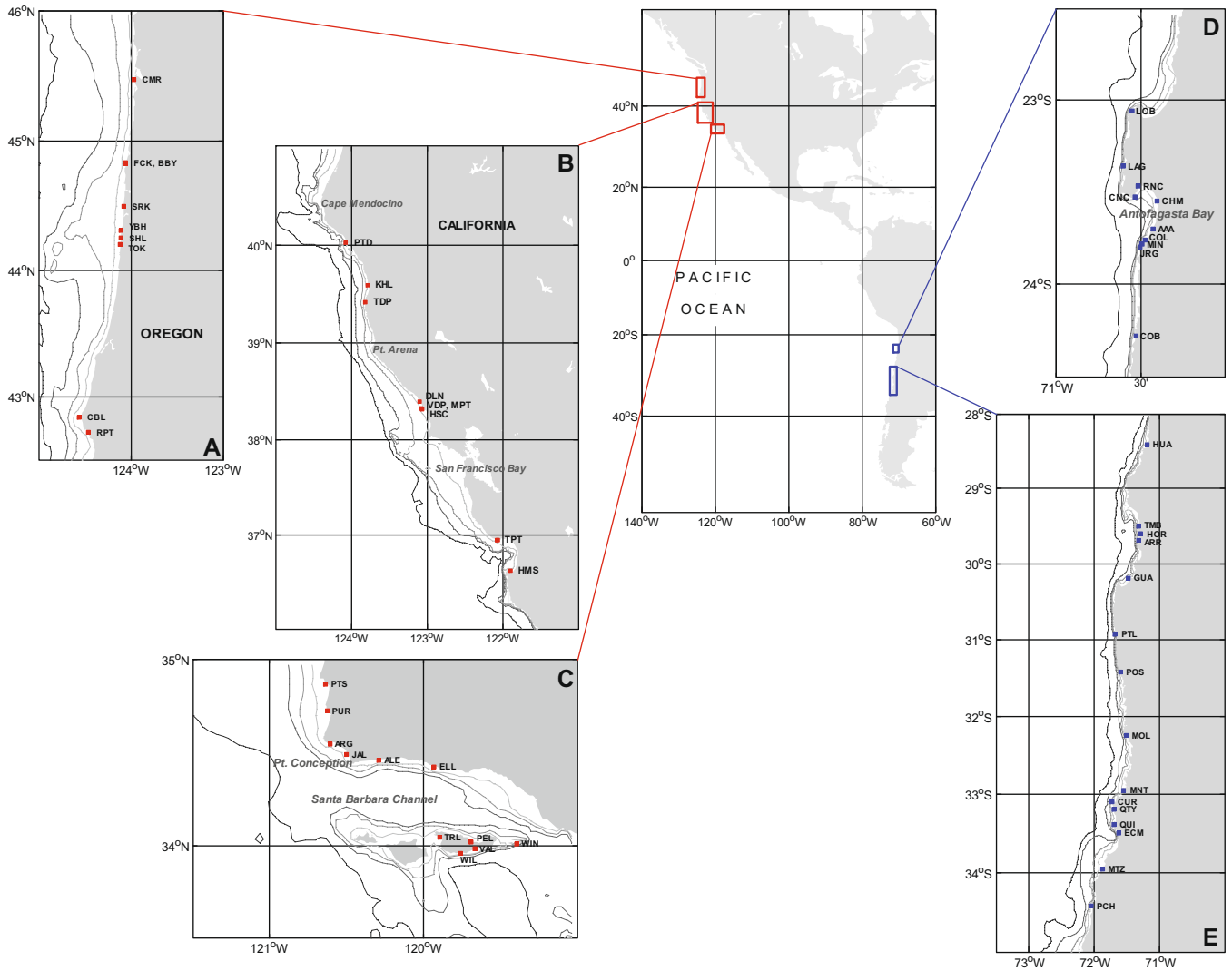


Fig. 1. Geographic location of intertidal and subtidal sites along the coast of Oregon (A), California (B and C), and Chile (D and E), from which SST data were collected. Contours correspond to 50, 100, 200, and 1000 m isobaths.

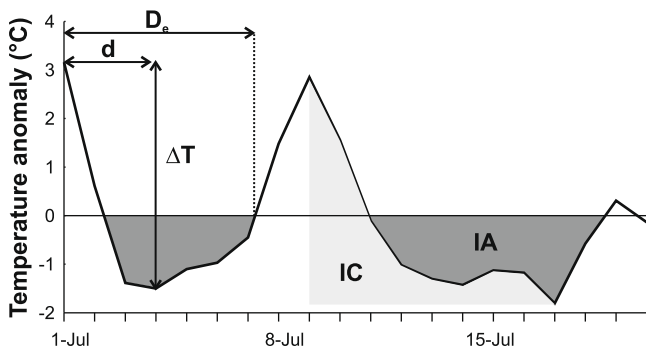


Fig. 2. Schematic of a daily SST anomaly time series segment covering two upwelling events, showing the metrics that were calculated for each event of anomalously cold water within each season and site. See Section 2 for explanation of terms.

3. *Integrated cooling IC.* An integrated measure of cooling, including both the range of temperature drop ΔT and the duration of the low temperatures d , calculated as the area under the anomaly curve during the cooling phase (light gray area in Fig. 2). *IC* can be scaled by $\Delta T d / 2$ so that the temperature drop can be scaled by $(2CR * IC)^{1/2}$ and duration can be scaled by $(2IC / CR)^{1/2}$.

4. *Integrated anomaly IA.* An integrated measure of the upwelling event, including both the duration of the anomaly and the intensity of it, calculated as the area between the anomaly curve and the zero line during the cold phase (dark gray area in Fig. 2). The intensity of the anomaly is reasonably scaled by IA / D_e .

Seasonal measures of event duration and cooling rate were obtained by averaging over all events to get a mean duration and mean cooling rate for a given season and site

$$\overline{D_e} = \frac{1}{E} \sum_{t=1}^E D_e \quad \overline{CR} = \frac{1}{E} \sum_{t=1}^E CR$$

where E is the number of events observed during that season. Similarly, seasonal measures of integrated cooling and integrated anomaly were obtained by summing over all events to get a measure of total integrated cooling and total integrated anomaly for a given season and site

$$TIC = \sum_{t=1}^E IC \quad TIA = \sum_{t=1}^E IA$$

Based on these metrics $\overline{D_e}$, \overline{CR} , TIC and TIA, which measure different but correlated aspects of cold events, together with the spatial anomaly in temperature at each site (T_r), we conducted a principal component analysis to classify each site-season. We used both the first and second principal component axes of this Multivariate Upwelling Zone Index of Cooling (MUZIC1 and MUZIC2) as a quantitative measure of upwelling-driven temperature variability for each site-season.

To compare latitudinal patterns produced by our multivariate index, and to highlight differences in spatial resolution with existing upwelling indices, we used Offshore Ekman Transport (OET) estimates (i.e. Bakun index) produced with a 1° spatial resolution by the Pacific Fisheries Environmental Laboratory (<http://www.pfeg.noaa.gov/>) for the period 1999–2007. Six-hourly OET series were used to compute daily series, which were integrated over each spring–summer season (see above). Mean cumulative spring–summer OET were then calculated for each latitude.

Finally, to illustrate the applicability of multivariate indices as environmental correlates for among-site differences in biological traits, we compared their spatial pattern of variability with changes in biomass of corticated algae and growth rate of one species (*Gelidium chilense*). Biomass (growth rate) observations were conducted during the same year at 13 (8) rocky intertidal sites encompassing 500 km of shoreline along central Chile (PCH to TMB, see Fig. 1e and supplementary information Table A2). Previous studies (Wieters, 2005) have shown that these algae can respond to changes in nutrient supply produced by meso-scale variation in upwelling intensity (see also Nielsen and Navarrete, 2004). Corticated algal biomass was estimated in the field following Wieters et al. (2009), whereas growth rate was measured according to Wieters (2005).

3. Results

3.1. SST variability and upwelling statistics

Daily series of mean SST calculated from the *in situ* records showed varying degrees of seasonality across regions (Fig. 3). Short-term summertime oscillations indicative of upwelling/relaxation cycles were coherent over tens to hundreds of kilometers, with significant zero-lag correlations for sites located up to 200 km apart (see Fig. A1 in Supplementary Information), and were most apparent at higher-latitude sites (Fig. 3f–h and n–p).

Univariate indices of thermal variability calculated for each site are shown in Tables A3 and A4 (Supplementary information). Cooling events ranged in mean duration (D_e) between 9.5–21.3 d for California–Oregon sites and 8.8–15.7 d for Chilean sites, with mean temperature drops (ΔT) ranging between 1.63–3.85 °C and 1.67–2.80 °C, respectively (see Tables A3 and A4 in Supplementary Information). Correlations between inter-annual means of these univariate metrics and the latitude-corrected SST (T_r) are shown in Table 1. In the northern hemisphere (Table 1A), the average cooling rate (CR) was positively and significantly correlated with time-integrated intensities of cooling (TIC) and negative-anomaly events (TIA), which were not correlated with the mean duration of cold events (D_e), suggesting that among-site differences in cooling rate are due to differences in the amplitude rather than duration of temperature drops. Cooling rates were negatively correlated with the mean duration of cold events (D_e), indicating that longer negative-anomaly events were associated with less abrupt drops in surface temperature (Table 1A). A somewhat similar structure among these four indices was observed for sites along the coast of Chile (Table 1B), where TIC and TIA were significantly and negatively correlated with the latitude-corrected mean SST

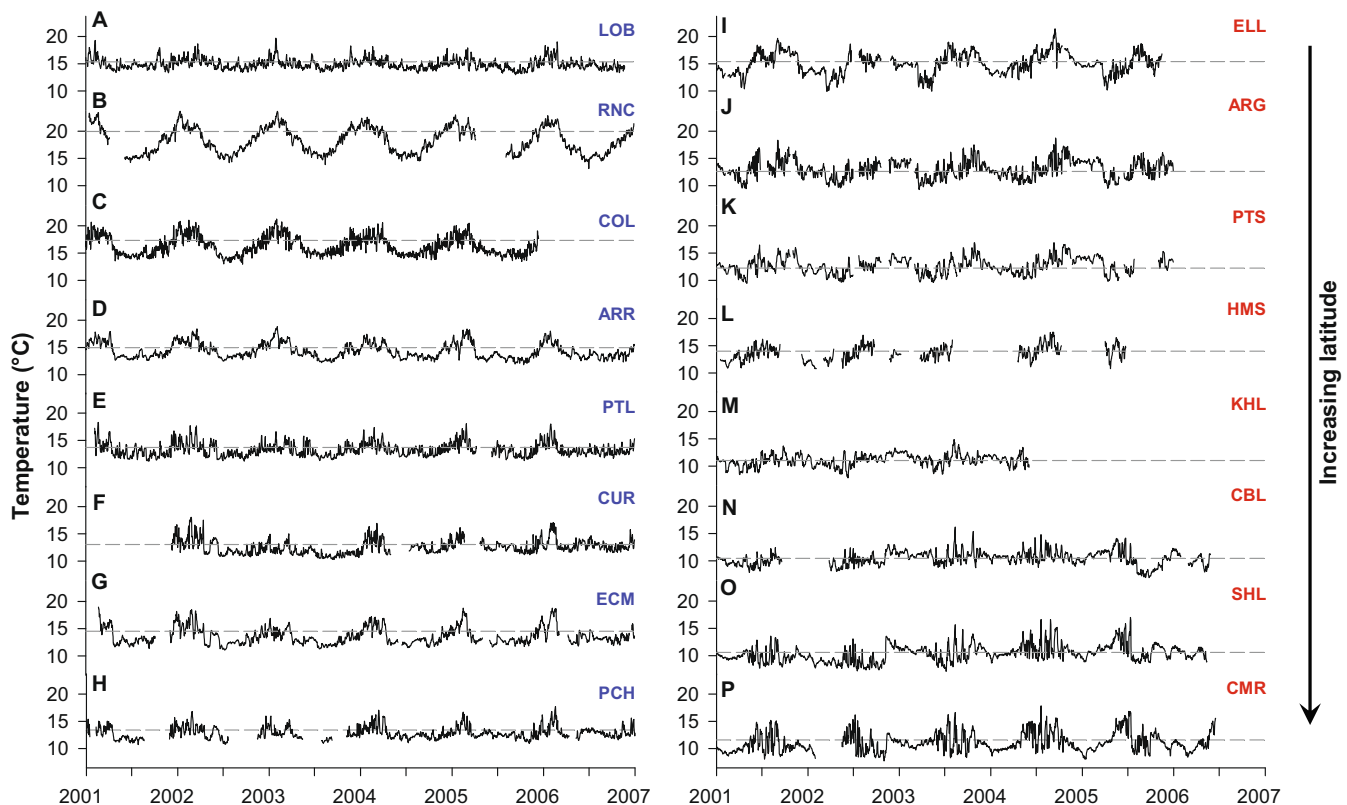


Fig. 3. Subset of the daily mean SST time series used in the analysis, which were gathered from *in situ* records along the coast of Chile (A–H), California (I–M), and Oregon (N–P). Dashed lines correspond to the long-term mean SST for each site. See Tables A1 and A2 (Supplementary information) for more details.

Table 1

Pearson correlation coefficients and associated probabilities (in parentheses) between inter-annual means of metrics based on daily SST anomalies from (A) 30 sites along the coast of Oregon–California (d.f. = 29), and (B) 25 sites along the coast of central and northern Chile (d.f. = 24). See Fig. 2 and text for explanation of terms. Significant values ($\alpha = 0.05$) are shown in boldface.

| | Latitude | T_r | D_e | CR | TIC |
|----------------------------------|-----------------------|------------------------|------------------------|-----------------------|-----------------------|
| <i>A. Oregon–California</i> | | | | | |
| D_e | 0.019 (0.919) | –0.293 (0.116) | | | |
| CR | 0.318 (0.086) | 0.009 (0.963) | – 0.574 (0.001) | | |
| TIC | 0.176 (0.354) | 0.114 (0.548) | –0.253 (0.178) | 0.563 (0.001) | |
| TIA | 0.398 (0.029) | –0.007 (0.972) | –0.241 (0.201) | 0.753 (<0.001) | 0.886 (<0.001) |
| <i>B. Central-Northern Chile</i> | | | | | |
| D_e | 0.659 (<0.001) | 0.179 (0.052) | | | |
| CR | –0.235 (0.258) | –0.147 (0.482) | – 0.621 (0.001) | | |
| TIC | 0.052 (0.804) | – 0.415 (0.039) | –0.313 (0.127) | 0.704 (<0.001) | |
| TIA | 0.201 (0.336) | – 0.461 (0.021) | –0.193 (0.354) | 0.680 (<0.001) | 0.925 (<0.001) |

(T_r), suggesting that sites with more intense temperature drops are also those where surface temperatures are lower than expected for their latitude (i.e. where upwelling is more persistent). Finally a positive correlation between D_e and latitude (Table 1B) suggests that negative-anomaly events increase in average duration as latitude increases (i.e. polewards) off Chile.

3.2. Among-site and inter-annual variability of univariate indices

When calculated separately for each spring–summer season, index values showed varying degrees of inter-annual consistency among sites (Fig. 4). From the subset of sites shown on Fig. 3, those located near known points of persistent upwelling were always colder than expected for their respective latitudes (e.g. PTS, ARG, LOB, PTL, CUR – Fig. 4f, g, i, m, and n). On the other hand, positive T_r values were found at sites where nearshore retention of warm surface waters has been documented (e.g. RNC, ECM – Fig. 4j and o). While both CR and TIC remained within narrow ranges at most sites on the Chilean coast (Fig. 4i–p), sites on the California–Oregon coast showed wider inter-annual fluctuations in cooling intensity (Fig. 4b, c, and f) and cooling rate (Fig. 4a and h). Finally, all three indices varied widely from year to year at ELL (Fig. 4h), a site located in the Santa Barbara Channel, south of Pt. Conception (Fig. 1c), where temperature variability in the water column is strongly influenced by processes other than coastal upwelling (i.e. seasonal cycle in stratification, local topography, and internal waves, see Cudaback et al., 2005).

Inter-annual means of the same univariate indices were used to produce a first ordination of sites (Fig. 5). The resulting ordination indicated that a greater number of sites along the California–Oregon coast (Fig. 5a) tend to experience greater cooling intensity for a given cooling rate than sites along the Chilean coast (Fig. 5b). On this CR/TIC plane, there was no trend in the distribution of latitude-corrected mean temperature (T_r). Regardless of their combination of CR and TIC values, mean temperatures were lower than expected for their latitude (blue dots) at sites located near upwelling centers such as Pt. Conception (PTS, PUR, ARG – Fig. 5a) and the Mejillones Peninsula in central Chile (LOB, LAG – Figs. 5b and 1d). Sites located on the eastern side of Santa Cruz Island, southern California (WIN, PEL – Fig. 5a) showed the lowest cooling rates together with the most positive T_r . Three sites located inside the Bay of Antofagasta in northern Chile (CNC, CHM, RNC) were arranged in a gradient of decreasing intensity, decreasing cooling rate and increasing T_r towards RNC (Fig. 5b), which has been shown to lie within the “upwelling shadow” of Pt. Coloso

(COL, see Fig. 1d – Piñones et al., 2007). At the opposite end of this gradient, and consistent with the fact that they are well-known upwelling centers, COL and JRG, located ~35 km south of RNC, showed more intense and rapid cooling together with negative T_r (Fig. 5b). The intensity, rate of cooling, and latitude-corrected mean temperature observed for JRG were comparable to those found for Pt. Curaumilla (CUR), another well-known upwelling center located 1000 km to the south (Fig. 1e).

3.3. Multivariate indices and site classification

A Principal Components Analysis of the univariate indices produced two principal components (MUZIC1 and MUZIC2) that explained 59% and 24% of total variability. A scatterplot (ordination) of MUZIC1 and MUZIC2 scores (Fig. 6) allowed us to visualize spatial structure and compare sites and regions on the multivariate space of thermal metrics. No clear segregation was observed between the two ecosystems of United States (Fig. 6, black) and Chile (Fig. 6, gray). MUZIC1 effectively separated sites that are in close proximity but exhibit marked differences in thermal regimes, such as those lying within or next to the Bay of Antofagasta (COL, AAA, CNC, CHM, and RNC) or located around Santa Cruz Island (WIN, PEL, VAL, WIL – see Fig. 6a). Interestingly, sites from the Oregon and northern California coast grouped with well-documented upwelling centers from central and northern Chile (Fig. 6b). In addition, sites located near Pt. Conception (PTS, PUR, ARG, JAL) appeared to be characterized by substantially different thermal event regimes (Fig. 6a). This result highlights the potential for our multivariate indices to capture small-scale differences in local regimes of temperature variability, while at the same time allowing for comparisons across regions.

Latitudinal distributions of MUZIC1 indicated a drop in upwelling intensity with latitude for northern Oregon sites, from Cape Blanco (CBL) to Cape Meares (CMR), consistent with the trend shown by inter-annual means of the cumulative Offshore Ekman Transport (OET, Fig. 7a). The multivariate index varied widely among northern and southern California sites, which was in clear contrast with the spatial pattern shown by the mean cumulative OET (Fig. 7b and c). According to MUZIC1, upwelling-induced thermal variability decreases at sites around Pt. Conception, and increases towards the western side of Santa Cruz Island (Fig. 7c). Such small-scale structure was not resolved by cumulative OET for this sub-region (Fig. 7c). A similar degree of small-scale variability in thermal regimes was found for sites located inside and outside the Bay of Antofagasta, in northern Chile (Figs. 1d and

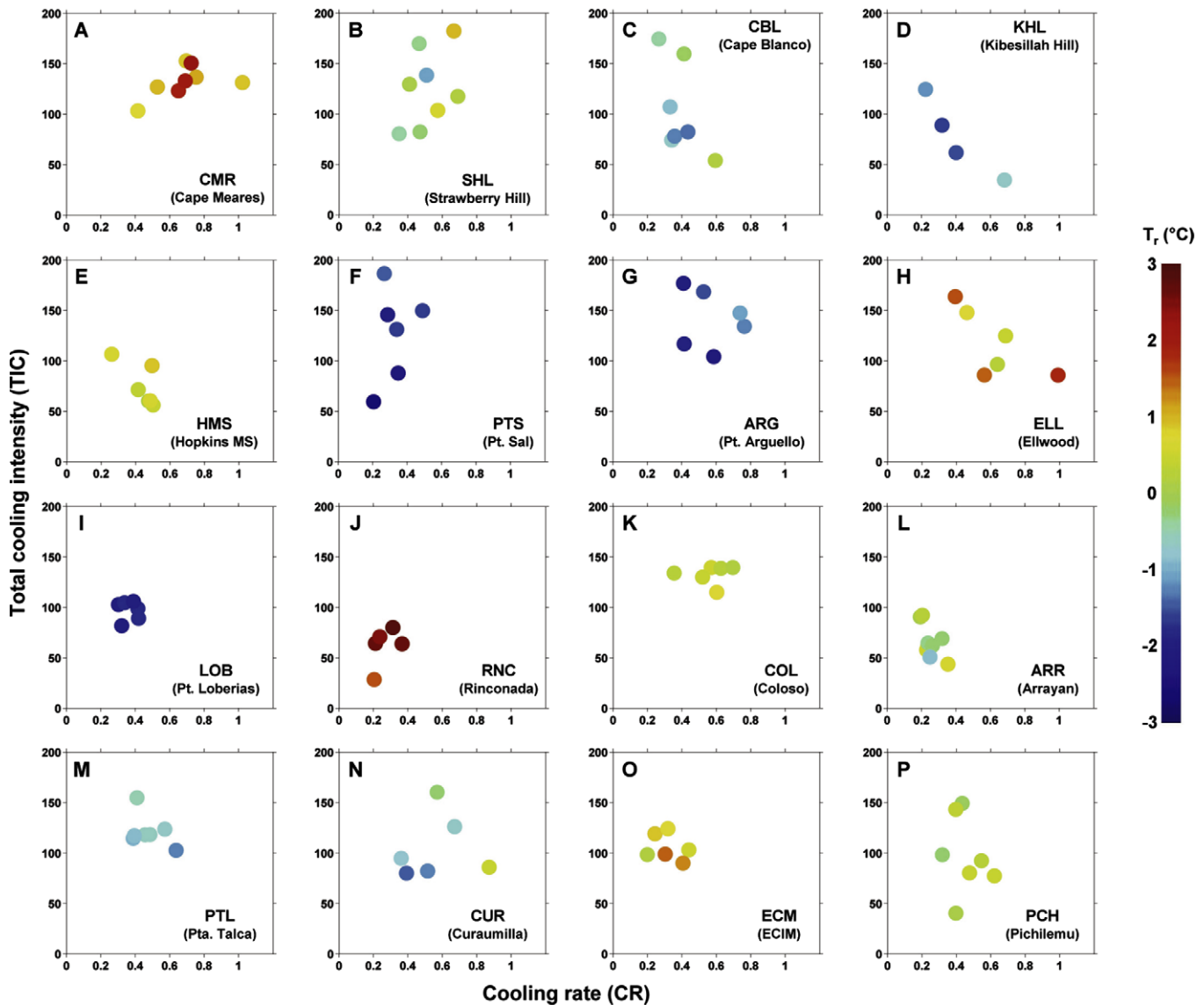


Fig. 4. Examples of inter-annual variability in three univariate indices (CR, TIC, and T_r) derived from daily time series of *in situ* Sea Surface Temperature at sites along the coast of Oregon (A–C), California (D–H), and Chile (I–P). Each panel corresponds to a site, and each point corresponds to a spring–summer season. The color scale corresponds to spatial SST residuals (T_r), which were calculated as the difference between mean spring–summer SST for each site and a latitudinal trend estimated by linear regression.

7d); this pattern was not reflected by the distribution of mean cumulative OET (Fig. 7d). MUZIC1 values for sites in central-northern Chile showed an apparent break in thermal regimes around 30.5°S (Fig. 7e). Mean cumulative OET for the 30–32°S region showed the highest inter-annual variability (Fig. 7e, dotted lines) and were nearly twice as high as those found for northern California (Fig. 7b, solid line).

3.4. Index application

Significant correlations were found between each of the three univariate indices and the total biomass of corticated algae (Fig. 8a–c). Higher biomass was correlated with faster and more intense cooling, as well as with negative values of latitude-corrected mean SST. While none of the univariate indices (CR, TIC, and T_r) explained more than 50% of among-site variance when used separately as predictors for corticated algal biomass (Fig. 8a–c), the multivariate index MUZIC1 explained 59% of total variance (Fig. 8d). The opposite was true for growth rates of *G. chilense*. Cooling rate alone explained 73% of total among-site

variance in growth rates (Fig. 8f), whereas marginally significant correlations that explained 52% and 50% of among-site variance were obtained for MUZIC1 and MUZIC2, respectively (Fig. 8i and j).

4. Discussion

Our results show that univariate and multivariate indices of *in situ* temperature variability produced by synoptic-scale events can capture small-scale differences in regimes of environmental variability, which appear to be driven largely by the modulation of upwelling by topography and coastline orientation (Kirincich et al., 2005; Broitman and Kinlan, 2006). These differences can be substantial between sites located in close proximity, at distances that are well beyond the spatial resolution of the Bakun index (Bakun, 1973; Pickett and Schwing, 2006). Although, the spatial resolution of currently available SST satellite imagery (up to 1 km) makes it possible to monitor inner-shelf temperatures at scales comparable to those presented here, obtaining gap-free daily time series of

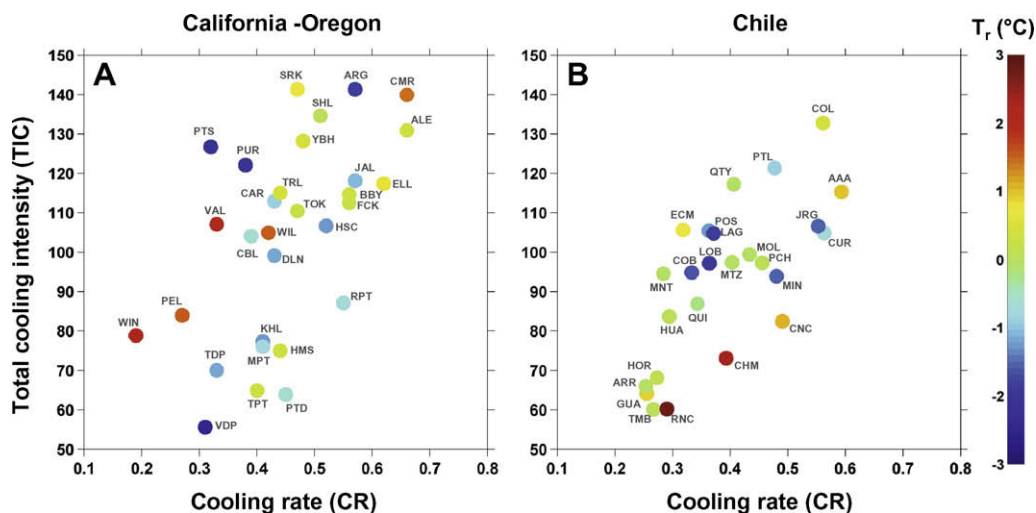


Fig. 5. Ordination of sites along the United States west coast (A) and the coast of Chile (B) based on the inter-annual means of three univariate indices. Axes and color scales as in Fig. 4. See Tables A1 and A2 in Supplementary information for site codes.

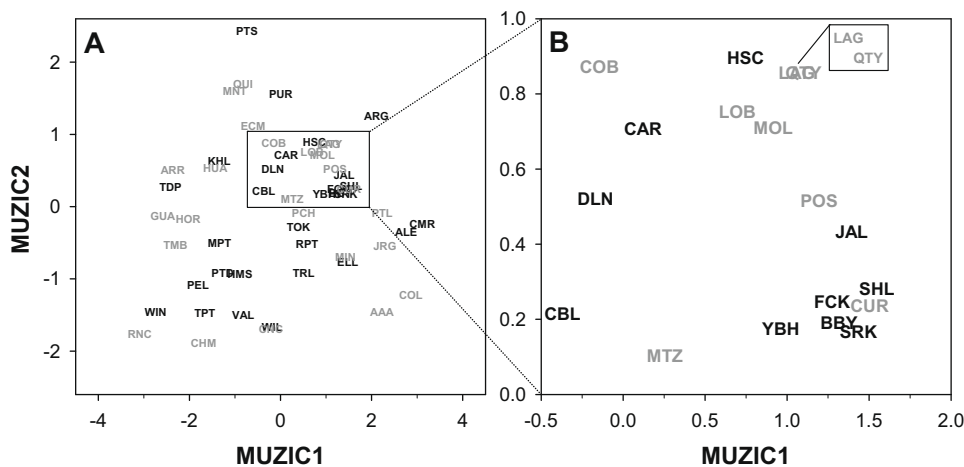


Fig. 6. (A) Ordination of sites along the US West coast (black) and the coast of Chile (gray) based on MUZIC1 and MUZIC2, the first two principal components of a Principal Components Analysis performed with univariate indices derived from daily time series of *in situ* Sea Surface Temperature. (B) Detail of the section marked with a black rectangle in (A). See Tables A1 and A2 in Supplementary information for site codes.

satellite SST for a given location (i.e. pixel) is often precluded by cloud cover and/or poor data quality in the nearshore. Composite images have thus been used to compute SST anomalies at a lower temporal resolution (e.g. Roy et al., 2001; Blanchette et al., *in press*). A comparison between index values computed with satellite-derived SST anomalies and those reported here will be the subject of a future publication.

Metrics of thermal variability presented in this paper differ from existing indices of upwelling (e.g. Bakun, 1973; Thomson and Ware, 1996; Santos et al., 2001) in that they are not meant to produce a shoreline proxy for upwelling on an event-by-event basis, or to establish spatial-temporal scales at which specific upwelling pulses modulate coastal SST (e.g. Roy et al., 2001) or elicit a biological response in the water column (e.g. Wang and Walsh, 1976). Instead, we sought to provide a physical correlate for biological properties that are likely to “integrate” temporal variability in environmental conditions, such as growth rates of benthic algae and invertebrates (Phillips, 2005; Blanchette et al., 2006; Wieters et al., 2009).

The simple univariate indices described here provide valuable information as to different aspects of thermal variability, and

would allow researchers a more mechanistic and quantitative understanding of the physical environment and its effects on biological processes and community structure (see Blanchette et al., *in press*). While the total intensity of cooling (TIC) could be a proxy for upwelling intensity upstream of a given site, the tendency for a site to be cooler than expected for its latitude (i.e. $T_r < 0$) appears to reflect its exposure to more persistent upwelling, particularly if long time series are used. On the other hand, positive values (i.e. a site tends to be warmer than expected for its latitude) are probably the result of retentive flows in the nearshore and/or frequent downwelling. Anomalous warm waters may result from the interaction of mesoscale wind patterns and coastal topography as shown for the bays of Antofagasta and Cartagena in northern and central Chile (Kaplan et al., 2003; Narváez et al., 2004, 2006; Piñones et al., 2007). Finally, the rate of cooling at a site (CR) could also be determined by local bathymetry and shoreline orientation relative to prevailing winds and/or coastal flows, as suggested by the sharp change in CR observed for three neighboring sites located inside the Bay of Antofagasta (RNC, CHM, CNC – Fig. 5b and 1d), and for three sites around Santa Cruz Island (WIN, PEL, VAL – Fig. 5a and 1c).

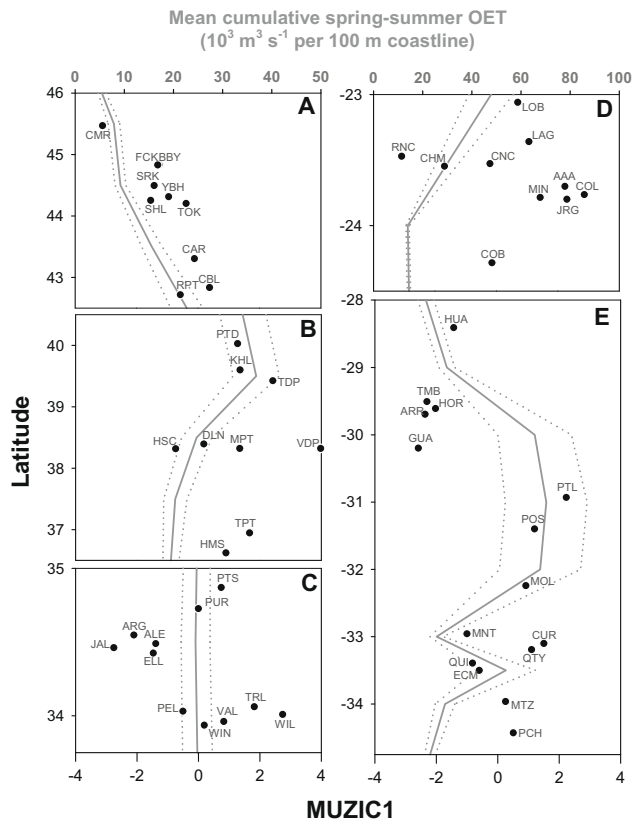


Fig. 7. Latitudinal distribution of the multivariate index MUZIC1 calculated using metrics derived from daily time series of *in situ* SST at sites along the coast of Oregon (A), California (B and C) and Chile (D and E). Solid gray lines correspond to inter-annual means (\pm SE, dashed lines) of the cumulative Offshore Ekman Transport (i.e. Bakun index) computed over spring–summer months for 1999–2007. Note the different scales for panels A–C and D–E. See Tables A1 and A2 in Supplementary information for site codes.

4.1. Persistence of local regimes of temperature variability

A site-by-site inspection of inter-annual variability in the three univariate indices (Fig. 4) made it possible to assess the persistence

of local regimes of temperature. If thermal variability is heavily dependent on local coastline orientation and bathymetry, metrics for a site might not change drastically from year to year. Although that was the case for several sites on the northern and central Chile coast (Fig. 4i–k and o), cooling rate and intensity varied widely at most California and Oregon sites (Fig. 4a–h). Latitude-corrected mean temperatures (T_r), on the other hand, were consistently negative at sites known to be affected by persistent upwelling (Fig. 4f, g, i, and m), and positive at sites where the interaction of wind forcing and local topography or mesoscale circulation patterns induces the retention of warm surface waters near the shoreline (Fig. 4h, j, and o). Thus, it appears that under certain conditions (i.e. coastal configuration and its interaction with mesoscale forcing) these univariate metrics are sufficient to quantitatively characterize the thermal regime perceived by a site.

4.2. Among-site and inter-hemisphere variation

The site ordinations produced by univariate and multivariate indices were consistent with existing knowledge as to (1) the degree to which temperature variability at some sites is driven by coastal upwelling and (2) the heterogeneity that is possible to observe in local regimes of SST variability. For instance, the inter-annual consistency of negative residual SST (T_r) calculated for sites located just north of Pt. Conception (PTS, PUR, ARG – Fig. 1c and 4a) is consistent with recent records of inner-shelf circulation and temperature variability that indicate persistent upwelling through most of the spring–summer season (Cudaback et al., 2005). Comparable cooling rates and intensities but varying degrees of persistence were found for central Oregon sites (SRK, SHL, YBH – Fig. 1 and 4a), where inner-shelf currents respond to more intermittent upwelling-favorable winds (Kirincich et al., 2005). Similar degrees of persistence but cooling intensities lower than those found for Pt. Conception sites were observed at COB, LOB, LAG, and JRG (Fig. 1d and 4b), all of which are located near upwelling centers around the Bay of Antofagasta (Lagos et al., 2002; Piñones et al., 2007). The multivariate ordination group Pt. Curaumilla (CUR), an upwelling center in central Chile (Fonseca and Farías, 1987; Sievers and Vega, 2000; Aiken et al., 2008), with central Oregon sites such as Strawberry Hill (SHL), Seal Rock (SRK),

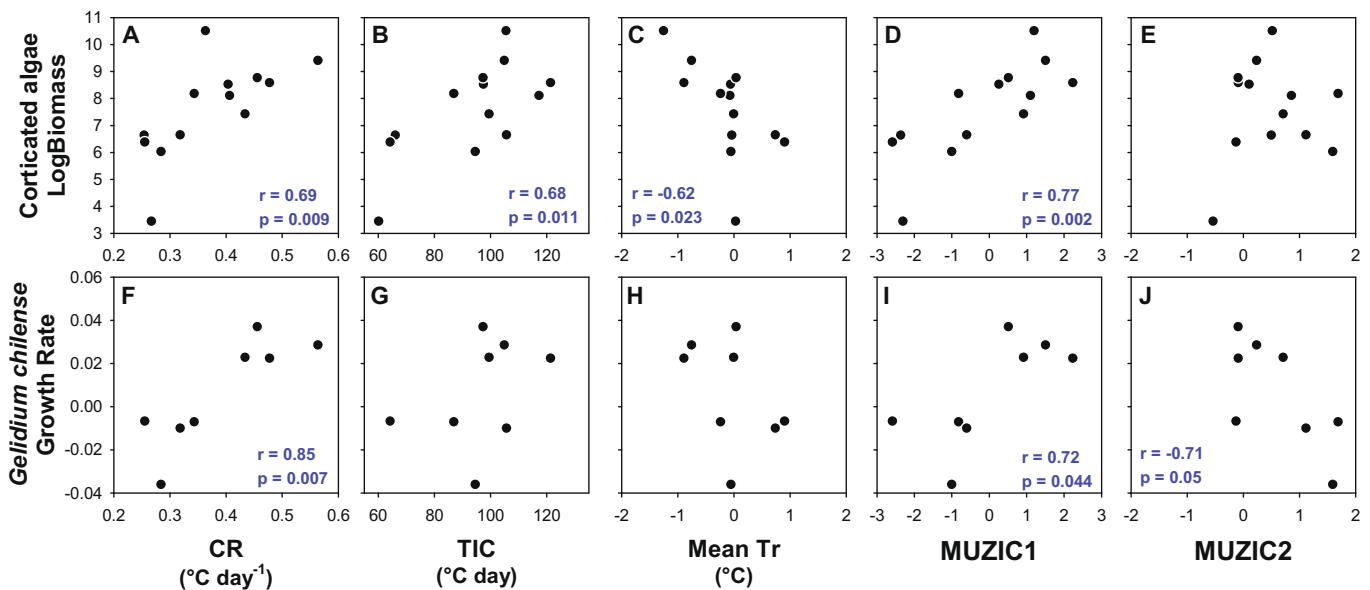


Fig. 8. Correlations between small-scale indices of thermal variability and (A–E) total biomass of corticated intertidal macro-algae and (F–J) growth rates estimated for the corticated alga *Gelidium chilense*. Observations to estimate biomass and growth rates were conducted during the same upwelling season at 13 and 8 sites, respectively, encompassing 500 km of shoreline along central Chile (see Table A2).

Boiler Bay (BBY), and Fogarty Creek (FCK, Fig. 6). As for small-scale heterogeneity in thermal regimes, we found examples of substantial differences in the value of univariate and multivariate indices for sites separated by short distances in topographically complex areas. For example, the full range of CR and TIC values was spanned by four sites distributed over ca. 40 km of shoreline around the Bay of Antofagasta (RNC, CHM, AAA, COL – Fig. 5b), whereas two sites separated by a similar distance across the Santa Barbara Channel (PEL, ELL – Fig. 1c) spanned the full range of CR and approximately half the range of TIC values found for California–Oregon sites (Fig. 5a). It is possible that some of this small-scale structure is due to thermal variability induced by sub-mesoscale features, such as the coastal eddies observed in the Santa Barbara Channel (Bassin et al., 2005).

Our PCA-based site ordination (MUZIC) considering both hemispheres (Fig. 6) highlights the potential of a multivariate-index approach to capture consistent similarities and differences in thermal regimes across different regions of the world. This type of analysis will aid in the design of inter-hemispheric studies where community attributes and vital rates are compared among sites with similar regimes of environmental variability. It is also promising that the univariate and MUZIC indices captured features of local thermal variability that were well correlated to algal biomass and growth rates measured at sites encompassing 500 km of the central Chile shoreline. Previous studies have shown that these algae can respond to changes in nutrient concentrations produced by meso-scale variation in upwelling intensity (Nielsen and Navarrete, 2004; Wieters, 2005). Interestingly, a simple univariate index like CR appeared to perform better than MUZIC indices as predictor for algal growth rates (Fig. 8f), whereas the multivariate MUZIC1 explained over 10% more among-site variance in corticated algal biomass than any single univariate index (Fig. 8b). Further studies should examine whether the indices can explain variation in other benthic algal groups as well as coastal phytoplankton productivity.

It is encouraging that, for areas spanning nearly 3° and 7° of latitude along the Oregon and central Chile coast, the latitudinal distribution of MUZIC1 roughly resembles that of the cumulative Bakun index (Fig. 7a, e). This suggests that time-integrated variability of inner-shelf temperatures could be a proxy for net offshore transport in certain regions. North-central Chile stands out among the five sub-regions considered in this study for its combination of an approximately north–south linear shoreline and extremely narrow continental shelf (Fig. 1). Future analyses must be conducted to establish whether this combination of topographic features determines a better mapping of mesoscale atmospheric forcing onto small-scale regimes of thermal variability.

Clearly, causal connections between local changes in temperature and particular aspects of the coastal upwelling process (e.g. alongshore advection, vertical flows, nutrient inputs, frontal structure, topographic enhancement, etc.) cannot be drawn without measurements of other physical processes. Datasets on wind variability from coastal buoys and satellite-borne sensors such as QuikSCAT may now be combined to provide a record of coastal wind stress with enough spatial resolution in some regions to help tease apart the different instances in which cold waters may be advected into a coastal site (e.g. Cudaback et al., 2005; Woodson et al., 2007). Furthermore, extensive datasets of inner-shelf current velocities measured by moored ADCPs are available for at least 10 of the California and Oregon sites presented here (e.g. Kirincich et al., 2005). Estimates of surface and bottom transport derived from these data, their correlation with coastal wind stress, and their potential correlation with the univariate and multivariate indices presented here will be part of a future publication.

Acknowledgements

This contribution is the result of numerous discussions and collaborative work by a large group of scientists from the ICORUMBA Consortium, funded by the Andrew Mellon Foundation. Discussions with Brian Kinlan, Steven Gaines, George Branch, Ruth Branch, Maya Pfaff, Chris Aiken, Carol Blanchette, Samuel Hormazabal, Rene Garreaud, and Melanie Fewings were most helpful. Christopher Krenz and Tess Freidenburg provided some of the northern California temperature. Comments by Allan Boyd and two other (anonymous) reviewers substantially improved this manuscript. FT was supported by a post-doctoral fellowship from the Andrew W. Mellon Foundation, and by a FONDECYT post-doctoral Grant (3070014). SAN and JCC acknowledge support from Grant FONDAP-FONDECYT 15001-001 to the Center for Advanced Studies in Ecology and Biodiversity. Additional funds for analysis and the preparation of this manuscript were provided by FONDECYT Grant 10730335 to SAN.

Appendix A. Supplementary data

Supplementary data associated with this article can be found, in the online version, at [doi:10.1016/j.pocean.2009.07.035](https://doi.org/10.1016/j.pocean.2009.07.035).

References

- Aiken, C.M., Navarrete, S.A., Castillo, M.I., Castilla, J.C., 2007. Along-shore larval dispersal kernels in a numerical ocean model of the central Chilean coast. *Marine Ecology Progress Series* 339, 13–24.
- Aiken, C.M., Castillo, M.I., Navarrete, S.A., 2008. A simulation of the Chilean Coastal Current and associated topographic upwelling near Valparaíso, Chile. *Continental Shelf Research* 28, 2371–2381.
- Andrews, W., Hutchings, L., 1980. Upwelling in the southern Benguela Current. *Progress in Oceanography* 9, 1–88.
- Bakun, A., 1973. Coastal upwelling indices, west coast of North America, 1946–1971. US Dept. Commerce NOAA Technical Report NMFS-SSRF 671, pp. 1–103.
- Bakun, A., Nelson, C.S., 1991. The seasonal cycle of wind-stress curl in subtropical Eastern Boundary Current regions. *Journal of Physical Oceanography* 21, 1815–1834.
- Bassin, C.J., Washburn, L., Brzezinski, M.A., McPhee-Shaw, E., 2005. Sub-mesoscale coastal eddies observed by high-frequency radar: A new mechanism for delivering nutrients to kelp forests in the Southern California Bight. *Geophysical Research Letters* 32. doi:10.1029/2005GL023017.
- Bernal, P.A., Robles, F.L., Rojas, O., 1982. Variabilidad física y biológica en la región meridional del sistema de corrientes Chile–Perú. In: Castilla, J.C. (Ed.), *Bases Biológicas Para el Uso y Manejo de Recursos Naturales Renovables: Recursos Biológicos Marinos*. P. Universidad Católica de Chile, Santiago, Chile, pp. 75–102.
- Blanchette, C.A., Helmuth, B., Gaines, S.D., 2006. Spatial patterns of growth in the mussel, *Mytilus californianus*, across a major oceanographic and biogeographic boundary at Point Conception, California, USA. *Journal of Experimental Marine Biology and Ecology* 340, 126–148.
- Blanchette, C.A., Wieters, E.A., Broitman, B.R., Kinlan, B.P., Schiel, D.R., in press. Trophic structure and diversity in rocky intertidal upwelling ecosystems: a comparison of community patterns across California, Chile, South Africa and New Zealand. *Progress in Oceanography*, doi:10.1016/j.pocean.2009.07.038.
- Botsford, L.W., Moloney, C.L., Hastings, A., Largier, J.L., Powell, T.M., Higgins, K., Quinn, J.F., 1994. The influence of spatially and temporally varying oceanographic conditions on meroplanktonic metapopulations. *Deep Sea Research Part II* 41, 107–145.
- Broitman, B.R., Kinlan, B.P., 2006. Spatial scales of benthic and pelagic producer biomass in a coastal upwelling ecosystem. *Marine Ecology Progress Series* 327, 15–25.
- Chaigneau, A., Eldin, G., Dewitte, B., in press. Eddy activity in the four major upwelling systems from satellite altimetry (1992–2007). *Progress in Oceanography*. doi:10.1016/j.pocean.2009.07.012.
- Connolly, S.R., Menge, B.A., Roughgarden, J., 2001. A latitudinal gradient in recruitment of intertidal invertebrates in the northeast Pacific Ocean. *Ecology* 82, 1799–1813.
- Cudaback, C.N., Washburn, L., Dever, E., 2005. Subtidal inner-shelf circulation near Point Conception, California. *Journal of Geophysical Research* 110. doi:10.1029/2004JC002608.
- Cury, P., Roy, C., 1989. Optimal environmental windows and pelagic fish recruitment success in upwelling areas. *Canadian Journal of Fisheries and Aquatic Sciences* 46, 670–680.
- Diehl, J.M., Toonen, R.J., Botsford, L.W., 2007. Spatial variability of recruitment in the sand crab *Emerita analoga* throughout California in relation to wind-driven currents. *Marine Ecology Progress Series* 350, 1–17.

- Ebert, T.A., Russell, M.P., 1988. Latitudinal variation in size structure of the west coast purple sea urchin. *Limnology and Oceanography* 33, 286–294.
- Fonseca, T., Farías, M., 1987. Estudio del proceso de surgencia en la costa chilena utilizando percepción remota. *Investigación Pesquera (Chile)*, 34.
- Graham, W.M., Largier, J.L., 1997. Upwelling shadows as nearshore retention sites: the example of northern Monterey Bay. *Continental Shelf Research* 17, 509–532.
- Helmuth, B., Broitman, B.R., Blanchette, C.A., Gilman, S., Halpin, P., Harley, C.D.G., O'Donnell, M.J., Hoffman, G.E., Menge, B., Strickland, D., 2006. Mosaic patterns of thermal stress in the rocky intertidal zone: implications for climate change. *Ecological Monographs* 76, 461–479.
- Hormazábal, S., Shaffer, G., Letelier, J., Ulloa, O., 2001. Local and remote forcing of sea surface temperature in the coastal upwelling system off Chile. *Journal of Geophysical Research* 106, 16657–16671.
- Hormazábal, S., Shaffer, G., Leth, O., 2004. Coastal transition zone off Chile. *Journal of Geophysical Research* 109. doi:10.1029/2003JC001956.
- Kaplan, D.M., Largier, J.L., Navarrete, S., Guíñez, R., Castilla, J.C., 2003. Large diurnal temperature fluctuations in the nearshore water column. *Estuarine, Coastal and Shelf Science* 57, 385–398.
- Kirincich, A.K., Barth, J.A., Menge, B.A., Lubchenco, J., 2005. Wind-driven inner-shelf circulation off central Oregon during summer. *Journal of Geophysical Research* 110. doi:10.1029/2004JC002611.
- Lagos, N.A., Barria, I.D., Paolini, P., 2002. Upwelling ecosystem of Northern Chile: integrating benthic ecology and coastal oceanography through remote sensing. In: Castilla, J.C., Largier, J.L. (Eds.), *The Oceanography and Ecology of the Nearshore and Bays in Chile*. Edic. Universidad Católica de Chile, Santiago, pp. 117–141.
- Lagos, N.A., Tapia, F.J., Navarrete, S.A., Castilla, J.C., 2007. Spatial synchrony in the recruitment of intertidal invertebrates along the coast of central Chile. *Marine Ecology Progress Series* 350, 29–39.
- Lentz, S.J., 1992. The surface boundary layer in coastal upwelling regions. *Journal of Physical Oceanography* 22, 1517–1539.
- Longhurst, A., 1998. *Ecological Geography of the Sea*. Academic Press, San Diego, CA.
- Mann, K.H., Lazier, J.R.N., 1996. *Dynamics of marine ecosystems*, 2nd ed.. Biological-Physical Interactions in the Ocean Blackwell Science, Malden.
- Marín, V.H., Delgado, L.E., Luna-Jorquera, G., 2003. S-chlorophyll squirts at 30°S off the Chilean coast (eastern South Pacific): Feature-tracking analysis. *Journal of Geophysical Research* 108. doi:10.1029/2003JC001935.
- McPhee-Shaw, E.E., Siegel, D.A., Washburn, L., Brzezinski, M.A., Jones, J.L., Leydecker, A., Melack, J., 2007. Mechanisms for nutrient delivery to the inner shelf: observations from the Santa Barbara Channel. *Limnology and Oceanography* 52, 1748–1766.
- Mendelssohn, R., Schwing, F.B., 2002. Common and uncommon trends in SST and wind stress in the California and Peru–Chile current systems. *Progress in Oceanography* 53, 141–162.
- Menge, B.A., Daley, B.A., Wheeler, P.A., Strub, P.T., 1997. Rocky intertidal oceanography: an association between community structure and nearshore phytoplankton concentration. *Limnology and Oceanography* 42, 57–66.
- Menge, B.A., Chan, F., Lubchenco, J., 2008. Response of a rocky intertidal ecosystem engineer and community dominant to climate change. *Ecology Letters* 11, 151–162.
- Montecinos, A., Pizarro, O., 2005. Interdecadal sea surface temperature–sea level pressure coupled variability in the South Pacific Ocean. *Journal of Geophysical Research* 110. doi:10.1029/2004JC002743.
- Moreno, C.A., Ascencio, G., Duarte, W.E., Marín, V., 1998. Settlement of the muricid *Concholepas concholepas* and its relationship with El Niño and coastal upwelling in southern Chile. *Marine Ecology Progress Series* 167, 171–175.
- Narváez, D., Poulin, E., Leiva, G., Hernandez, E., Castilla, J.C., Navarrete, S.A., 2004. Seasonal and spatial variation of nearshore hydrographic conditions in central Chile. *Continental Shelf Research* 24, 279–292.
- Narváez, D.A., Navarrete, S.A., Largier, J., Vargas, C.A., 2006. Onshore advection of warm water, larval invertebrate settlement, and relaxation of upwelling off central Chile. *Marine Ecology Progress Series* 309, 159–173.
- Navarrete, S.A., Broitman, B., Wieters, E.A., Finke, G.R., Venegas, R.M., 2002. Recruitment of intertidal invertebrates in the southeast Pacific: interannual variability and the 1997–1998 El Niño. *Limnology and Oceanography* 47, 791–802.
- Navarrete, S.A., Wieters, E.A., Broitman, B.R., Castilla, J.C., 2005. Scales of benthic–pelagic coupling and the intensity of species interactions: from recruitment limitation to top-down control. *Proceedings of the National Academy of Sciences, USA* 102, 18046–18051.
- Navarrete, S.A., Broitman, B.R., Menge, B., 2008. Interhemispheric comparison of recruitment to intertidal communities: pattern persistence and scales of variation. *Ecology* 89, 1308–1322.
- Nielsen, K.G., Navarrete, S.A., 2004. Mesoscale regulation comes from the bottom-up: intertidal interactions between consumers and upwelling. *Ecology Letters* 7, 31–41.
- Pérez-Brunius, P., López, M., Parés-Sierra, A., Pineda, J., 2007. Comparison of upwelling indices off Baja California derived from three different wind data sources. *CalCOFI Reports* 48, 204–214.
- Phillips, N.E., 2005. Growth of filter-feeding benthic invertebrates from a region with variable upwelling intensity. *Marine Ecology Progress Series* 295, 79–89.
- Pickett, M.H., Paduan, J.D., 2003. Ekman transport and pumping in the California Current based on the US Navy's high-resolution atmospheric model (COAMPS). *Journal of Geophysical Research* 108, 3327.
- Pickett, M.H., Schwing, F.B., 2006. Evaluating upwelling estimates off the west coasts of North and South America. *Fisheries Oceanography* 15, 256–269.
- Pineda, J., 2000. Linking larval settlement to larval transport: assumptions, potentials, and pitfalls. In: Färber-Lorda, J. (Ed.), *Oceanography of the Eastern Pacific*, vol. 1. CICESE, Ensenada, pp. 84–105.
- Pineda, J., Hare, J.A., Sponaugle, S., 2007. Larval dispersal and transport in the coastal ocean and consequences for population connectivity. *Oceanography* 20, 22–39.
- Piñones, A., Castilla, J.C., Guíñez, R., Largier, J.L., 2007. Nearshore surface temperatures in Antofagasta Bay (Chile) and adjacent upwelling centers. *Ciencias Marinas* 33, 37–48.
- Poulin, E., Palma, A.T., Leiva, G., Hernandez, E., Martinez, P., Navarrete, S.A., Castilla, J.C., 2002. Temporal and spatial variation in the distribution of epineustonic competent larvae of *Concholepas concholepas* along the central coast of Chile. *Marine Ecology Progress Series* 229, 95–104.
- Ramos, M., Pizarro, O., Bravo, L., Dewitte, B., 2006. Seasonal variability of the permanent thermocline off northern Chile. *Geophysical Research Letters* 33, L09608. doi:10.1029/2006GL025882.
- Roy, C., Weeks, S., Rouault, M., Nelson, G., Barlow, R., van der Lingen, C., 2001. Extreme oceanographic events recorded in the Southern Benguela during the 1999–2000 summer season. *South African Journal of Science* 97, 465–471.
- Santos, A.M.P., Borges, M.D.F., Groom, S., 2001. Sardine and horse mackerel recruitment and upwelling off Portugal. *ICES Journal of Marine Science* 58, 589–596.
- Scheuerell, M.D., Williams, J.G., 2005. Forecasting climate-induced changes in the survival of Snake River spring/summer Chinook salmon (*Oncorhynchus tshawytscha*). *Fisheries Oceanography* 14, 448–457.
- Shaffer, G., Pizarro, O., Djurfeldt, L., Salinas, S., Rutlant, J., 1997. Circulation and low-frequency variability near the Chilean coast: remotely forced fluctuations during the 1991–92 El Niño. *Journal of Physical Oceanography* 27, 217–234.
- Shaffer, G., Hormazábal, S., Pizarro, O., Salinas, S., 1999. Seasonal and interannual variability of currents and temperature over the slope of central Chile. *Journal of Geophysical Research* 104, 29951–29961.
- Shanks, A.L., Brink, L., 2005. Upwelling, downwelling, and cross-shelf transport of bivalve larvae: test of a hypothesis. *Marine Ecology Progress Series* 302, 1–12.
- Shanks, A.L., Roegner, G.C., 2007. Recruitment limitation in Dungeness crab populations is driven by variation in atmospheric forcing. *Ecology* 88, 1726–1737.
- Sievers, H., Vega, S., 2000. Respuesta físico-química de la bahía de Valparaíso a la surgencia generada en Punta Curaumilla y al fenómeno El Niño. *Revista de Biología Marina y Oceanografía* 35, 153–168.
- Strub, P.T., Mesias, J.M., Montecino, V., Rutlant, J., Salinas, S., 1998. Coastal ocean circulation off western South America. In: Robinson, A.R., Brink, K.H. (Eds.), *The Sea*, 11. John Wiley & Sons, New York, pp. 273–313.
- Thomson, R.E., Ware, D., 1996. A current velocity index of ocean variability. *Journal of Geophysical Research* 101, 14297–14310.
- Ulloa, O., Escribano, R., Hormazábal, S., Quiñones, R., Gonzalez, R., Ramos, M., 2001. Evolution and biological effects of the 1997–1998 El Niño in the upwelling ecosystem off northern Chile. *Geophysical Research Letters* 28, 1591–1594.
- Venegas, R.M., Strub, P.T., Beier, E., Letelier, R., Thomas, A.C., Cowles, T., James, C., Soto-Mardones, L., Cabrera, C., 2008. Satellite-derived variability in chlorophyll, wind stress, sea surface height, and temperature in the northern California Current System. *Journal of Geophysical Research* 113. doi:10.1029/2007JC004481.
- Wang, D.P., Walsh, J.J., 1976. Objective analysis of the upwelling ecosystem off Baja California. *Journal of Marine Research* 34, 43–60.
- Washburn, L., Swenson, M.S., Largier, J.L., Kosro, P.M., Ramp, S.R., 1993. Cross-shelf sediment transport by an anticyclonic eddy off Northern California. *Science* 261, 1560–1564.
- Wieters, E., 2005. Upwelling control of positive interactions over mesoscales: a new link between bottom-up and top-down processes on rocky shores. *Marine Ecology Progress Series* 301, 43–54.
- Wieters, E.A., Kaplan, D.M., Navarrete, S.A., Sotomayor, A., Largier, J., Nielsen, K.J., Veliz, F., 2003. Alongshore and temporal variability in chlorophyll *a* concentration in Chilean nearshore waters. *Marine Ecology Progress Series* 249, 93–105.
- Wieters, E., Broitman, B.B., Branch, G.M., 2009. Benthic community responses to spatio-temporal thermal regimes in two upwelling ecosystems: comparisons between South Africa and Chile. *Limnology and Oceanography* 54, 1060–1072.
- Woodson, C.B., Erkes-Medrano, D.I., Flores-Morales, A., Foley, M.M., Henkel, S.K., Hensing-Lewis, M., Jacinto, D., Needles, L., Nishizaki, M.T., O'Leary, J., Ostrander, C.E., Pespeni, M., Schwager, K.B., Tyburczy, J.A., Weersing, K.A., Kirincich, A.R., Barth, J.A., McManus, M.A., Washburn, L., 2007. Local diurnal upwelling driven by sea breezes in northern Monterey Bay. *Continental Shelf Research* 27, 2289–2302.